

# TMP21 Transmembrane Domain Regulates $\gamma$ -Secretase Cleavage<sup>\*[S]</sup>

Received for publication, August 25, 2009 Published, JBC Papers in Press, August 25, 2009, DOI 10.1074/jbc.M109.059345

Raphaëlle Pardossi-Piquard<sup>†1,2</sup>, Christopher Böhm<sup>‡2</sup>, Fusheng Chen<sup>‡</sup>, Soshi Kanemoto<sup>‡</sup>, Frédéric Checler<sup>§</sup>, Gerold Schmitt-Ulms<sup>†¶</sup>, Peter St. George-Hyslop<sup>‡||\*\*3</sup>, and Paul E. Fraser<sup>‡††4</sup>

From the <sup>†</sup>Centre for Research in Neurodegenerative Diseases, University of Toronto, Toronto, Ontario M5S 3H2, Canada, the <sup>§</sup>Institut de Pharmacologie Moléculaire et Cellulaire, CNRS, Equipe Labellisée Fondation pour la Recherche Médicale, Valbonne 06560, France, the <sup>¶</sup>Department of Laboratory Medicine and Pathobiology, University of Toronto, Toronto, Ontario M5S 1A8, Canada, the <sup>||</sup>Department of Medicine (Division of Neurology), Toronto Western Hospital Research Institute, University Health Network and <sup>††</sup>Department of Medical Biophysics, University of Toronto, Toronto, Ontario M5G 2M9, Canada, and the <sup>\*\*</sup>Department of Clinical Neuroscience, University of Cambridge, Cambridge CB2 0XY, United Kingdom

TMP21 has been shown to be associated with the  $\gamma$ -secretase complex and can specifically regulate  $\gamma$ -cleavage without affecting  $\epsilon$ -mediated proteolysis. To explore the basis of this activity, TMP21 modulation of  $\gamma$ -secretase activity was investigated independent of  $\epsilon$ -cleavage using an amyloid- $\beta$  precursor protein (APP $\epsilon$ ) construct which lacks the amyloid intracellular domain domain. The APP $\epsilon$  construct behaves similarly to the full-length precursor protein with respect to  $\alpha$ - and  $\beta$ -cleavages and is able to undergo normal  $\gamma$ -processing. Co-expression of APP $\epsilon$  and TMP21 resulted in the accumulation of membrane-embedded higher molecular weight A $\beta$ -positive fragments, consistent with an inhibition of  $\gamma$ -secretase cleavage. The APP $\epsilon$  system was used to examine the functional domains of TMP21 through the investigation of a series of TMP21-p24a chimera proteins. It was found that chimeras containing the transmembrane domain bound to the  $\gamma$ -secretase complex and could decrease  $\gamma$ -secretase proteolytic processing. This was confirmed through investigation of a synthetic peptide corresponding to the TMP21 transmembrane helix. The isolated TMP21 TM peptide but not the homologous p24a domain was able to reduce A $\beta$  production in a dose-dependent fashion. These observations suggest that the TMP21 transmembrane domain promotes its association with the presenilin complex that results in decreased  $\gamma$ -cleavage activity.

Alzheimer disease is a progressive neurodegenerative disorder and the most common cause of dementia worldwide. One

of the main histopathological hallmarks in Alzheimer disease is senile plaque, an extracellular protein deposit composed primarily of the amyloid  $\beta$ -peptide (A $\beta$ ),<sup>5</sup> which is generated by sequential cleavages of the amyloid- $\beta$  precursor protein (APP) by  $\beta$ - and  $\gamma$ -secretase activities (1). Cleavage by  $\gamma$ -secretase occurs within the APP transmembrane domain at several sequences, such as the  $\gamma$ -site, to produce A $\beta$ 40/42, and the  $\epsilon$ -site, which results in the release of the cytosolic amyloid intracellular domain (AICD) (2). AICD is targeted to the nucleus and regulates transcription of several genes including KAI1 (3, 4), glycogen synthase kinase 3 (4–6), neprilysin (7, 8), p53 (9), epidermal growth factor receptor (10), LRP1 (11), Tip60, APP, or  $\beta$ -site APP-cleaving enzyme (BACE) (4).

Several lines of evidence have shown that  $\gamma/\epsilon$ -secretase activity requires multimeric membrane protein complexes, the presenilin complexes, which are composed of at least four components: presenilin (PS1 or PS2), nicastrin (NCT), anterior pharynx-defective phenotype 1 (APH-1), and presenilin enhancer 2 (PEN-2) (12–16). All four components appear to be essential for  $\gamma/\epsilon$ -secretase activity (17–19). NCT and APH-1 form an initial subcomplex to which full-length PS1 or PS2 and PEN-2 are added (18, 20, 21). During maturation of the presenilin complexes, nicastrin is glycosylated, and presenilins are cleaved into N- and C-terminal fragments which remain associated as a heterodimer in the active high molecular weight complex (20, 22). In these complexes presenilins have been proposed to serve as the catalytic subunit (23), whereas the large ectodomain of NCT plays an essential role in substrate recognition (24, 25).

It has been demonstrated that TMP21, a member of p24 cargo protein with homology to p24a, binds the presenilin complexes and acts as a modulator resulting in the selective suppression of  $\gamma$ - but not  $\epsilon$ -secretase cleavage (26). TMP21 small interfering RNA suppression enhances the production of A $\beta$ , whereas overexpression or the ablation of TMP21 does not

\* This work was supported by grants from the Canadian Institutes of Health Research, Howard Hughes Medical Institute, Alzheimer Society of Ontario, The Ontario Research and Development Challenge Fund and the Canada Foundation for Innovation, the Fondation pour la Recherche Médicale, and the Conseil Général des Alpes Maritimes.

Author's Choice—Final version full access.

[S] The on-line version of this article (available at <http://www.jbc.org>) contains supplemental Fig. 1.

<sup>1</sup> Supported by the French National Research Agency. Current address: Institut de Pharmacologie Moléculaire et Cellulaire, CNRS, Equipe Labellisée Fondation pour la Recherche Médicale, Valbonne 06560, France.

<sup>2</sup> These authors contributed equally to this work.

<sup>3</sup> Supported by the Wellcome Trust.

<sup>4</sup> To whom correspondence should be addressed: Centre for Research in Neurodegenerative Diseases, University of Toronto, 6 Queen's Park Crescent West, Toronto, Ontario M5S 3H2, Tel.: 416 978-0102, Fax: 416 978-1878, E-mail: paul.fraser@utoronto.ca.

<sup>5</sup> The abbreviations used are: A $\beta$ , amyloid  $\beta$ -peptide; APP, amyloid- $\beta$  precursor protein; AICD, cytosolic amyloid intracellular domain; PS, presenilin; TM, transmembrane; NCT, nicastrin; WT, wild type; CHAPSO, 3-[(3-cholamidopropyl)dimethylammonio]-2-hydroxy-1-propanesulfonic acid; Tricine, N-[2-hydroxy-1,1-bis(hydroxymethyl)ethyl]glycine; NTF, N-terminal fragment; Nt, N terminus; Ct, C terminus; ELISA, enzyme-linked immunosorbent assay.

affect AICD production. In this context TMP21 has no effect on p53 or NEP, which are two target genes of AICD activation (27).

In the current study, the effects of TMP21 on  $\gamma$ -secretase activity were investigated independent of  $\epsilon$ -cleavage using an APP $\epsilon$  construct which lacks the AICD domain (terminates at A $\beta$ 49). The APP $\epsilon$  fragment behaves similarly to the full-length precursor protein with respect to  $\alpha$  and  $\beta$  cleavages and is able to undergo  $\gamma$ -processing, which is sensitive to inhibition by DFK167 (28). Co-expression of APP $\epsilon$  and TMP21 resulted in the accumulation of membrane-embedded higher molecular weight A $\beta$ -positive fragments, consistent with an inhibition of  $\gamma$ -secretase cleavage. This reporter system was used to determine the functional domain of TMP21 through the investigation of a series of TMP21-p24a chimera proteins. In addition, a synthetic peptide corresponding to the TMP21 transmembrane helix but not the p24a TM domain was able to reduce A $\beta$  secretion in a dose-dependent fashion. These observations indicate that the transmembrane domain of TMP21 is a primary site of action, and its physical association with the presenilin complex can alter  $\gamma$ -cleavage.

## EXPERIMENTAL PROCEDURES

**Mutagenesis and cDNA Constructs**—TMP21 and p24a tagged at the C-terminal with the FLAG epitope were cloned in pcDNA4 as previously described (26). Chimera constructs between TMP21 and p24a cDNA were obtained following a three-step PCR protocol as previously described (36), and then all constructs were confirmed by DNA sequencing and cloned in pcDNA4 vector with the FLAG epitope at the C terminus. APP $\epsilon$  constructs containing a stop codon at the end of the transmembrane domain of human APP (isoforms corresponding to 695 or 751) were cloned in pcDNA3 as previously described (28). The wild-type APP constructs (APP WT isoforms 695 or 751) were cloned into pcDNA3.

**Cell Culture, Transfection, and Treatment**—Native HEK293 cells or stably transfected HEK293 cells expressing the Swedish APP mutant (APPSwe) were maintained in Dulbecco's modified Eagle's medium (Invitrogen) supplemented with 10% fetal bovine serum. Transient transfections were performed in native HEK293 cells by using Lipofectamine 2000 (Invitrogen) or FuGENE 6 (Roche Applied Science) according to the manufacturer's instructions, and then cells were collected 24–48 h after transfection.

**Membrane Fraction Preparation and Immunoprecipitation**—HEK293 cells were harvested and homogenized in buffer A (5 mM HEPES, pH 7.4, 1 mM EDTA, 0.25 M sucrose, protease inhibitor mixture from Roche Applied Science). The homogenate was clarified by centrifugation at  $1000 \times g$  for 5 min at 4 °C, and the supernatant was centrifuged at  $100,000 \times g$  for 1 h at 4 °C. For immunoprecipitation of the intracellular A $\beta$  long species, cell pellets or membrane pellets were homogenized in radioimmune precipitation assay buffer (50 mM Tris, pH 7.4, 150 mM NaCl, 1 mM EDTA, 1% Triton, 0.5% deoxycholate, 0.1% SDS, protease inhibitor mixture). Isolates of either total lysate (2.5 mg) or membrane fraction (800  $\mu$ g) were diluted in 1 ml of radioimmune precipitation assay buffer. For immunoprecipitation of presenilin complexes, membrane pellets were homogenized in buffer B (25 mM HEPES, pH 7.4, 150 mM NaCl, 2 mM

EDTA, 1% CHAPSO, protease inhibitor mixture). Isolates of the membrane fraction (800  $\mu$ g) were diluted in 1 ml of buffer B to a final concentration of 0.5% CHAPSO. After preclearing with protein G-Sepharose 4 fast flow (GE Healthcare) for 1 h at 4 °C, lysates were subjected to immunoprecipitation with the appropriate antibody (a mouse monoclonal anti-A $\beta$  6E10 (from Covance) or a mouse monoclonal anti-FLAG (from Sigma) antibodies). Immunoprecipitants were recovered by overnight incubation at 4 °C with protein G-Sepharose. Beads were washed 3 times with radioimmune precipitation assay buffer or buffer B (0.5% CHAPSO) and once with phosphate-buffered saline.

**SDS/PAGE and Western Blot Analyses**—Whole cell lysates (total protein 50  $\mu$ g), membrane lysates (protein 25–50  $\mu$ g), and immunoprecipitated proteins were dissolved in SDS sample buffer, separated on Tris-Tricine gels 16% or Tris-glycine gels 4–20% (Invitrogen), and transferred to nitrocellulose membranes. Target proteins were visualized by enhanced chemiluminescence (ECL Amersham Biosciences) with the following antibodies: mouse monoclonal anti-A $\beta$  6E10 (Covance), anti-A $\beta$  4G8 (Covance), rabbit polyclonal anti-PS1-NTF, anti-NCT-Nt, anti-FLAG (from Sigma), and anti-APP CTF antibodies.

**Peptide Synthesis and Assays**—The TMP21 transmembrane domain sequence containing three N- and C-terminal lysine residues (KKK-VLYFSIFSMFLIGLATWQVFYL-KKK) and the p24a transmembrane domain (KKK-VVLSFFFEALVLVAMTLGQIYYL-KKK) peptides were synthesized by standard Fmoc (*N*-(9-fluorenyl)methoxycarbonyl)-based solid phase methodology. The terminal lysines were added to increase peptide solubility. Peptides were purified by reverse phase high pressure liquid chromatography using water/acetonitrile mixtures buffered with 0.1% trifluoroacetic acid on a POROS 20R2 column. Stock solutions of both peptides were prepared in DMSO and added at the desired final concentrations (10 and 30  $\mu$ g/ml) to the media of cultures of HEK293 cells stably expressing the Swedish variant of APP. Media was collected at different time points and A $\beta$ 40 levels were determined by ELISA.

**A $\beta$ 40 ELISA and Cell-free Assays**—A $\beta$ 40 levels were measured by ELISA assays using conditioned medium collected from HEK293 cells after a transient transfection or a treatment with synthetic peptide (TM-TMP21, TM-p24). The enzyme-linked immunoabsorbent assay ELISA was performed according to the manufacturer's instructions (BIOSOURCE). Determination of  $\gamma$ -secretase activity by cell-free assay was as previously described (26). Briefly, membrane fractions were isolated from HEK293 cells and incubated with recombinant FLAG-tagged APP-C100. TMP21 and p24a synthetic peptides solubilized in DMSO were added to the reaction mixture at the desired concentrations and A $\beta$ 40 generated by proteolysis was measured by ELISA.

**Statistical Analysis**—Statistical analyses were performed with PRISM software (Graph-Pad Software, San Diego, CA) by using the unpaired Student's *t* test for pairwise comparisons.

## RESULTS AND DISCUSSION

**Effects of TMP21 on  $\gamma$ -Secretase Processing in an APP $\epsilon$  Reporter Assay**—TMP21 is a type 1 transmembrane protein member of the p24 cargo-protein family that is involved in vesicular targeting and protein transport (29). In addition to its trafficking functions, TMP21 has been shown to specifically

## TMP21 Functional Domain

regulate proteolysis at the  $\gamma$ -secretase site, whereas no effects on  $\epsilon$ -cleavage were observed (26, 27, 30). A C-terminal-truncated APP construct terminating at the  $\epsilon$ -site was employed to allow investigation of TMP21 activity independent of  $\epsilon$ -medi-

ated cleavage (Fig. 1A). This APP $\epsilon$  protein is recognized by an A $\beta$  antibody targeting the N-terminal A $\beta$  residues 1–17 (6E10) (Fig. 1B) and undergoes normal processing by  $\alpha$ -,  $\beta$ -, and  $\gamma$ -secretase to produce similar levels of A $\beta$  peptides and soluble APP $\alpha$  (*sAPP $\alpha$* ) fragment in the absence of AICD production (Fig. 1, C and D). Comparable findings have been previously reported which confirm that the APP $\epsilon$  variant is comparable with the wild-type protein but permits examination of  $\gamma$ -secretase activities without any complicating factors associated with  $\epsilon$ -related processing (28).

Co-transfection of APP-WT or APP $\epsilon$  with C-terminal FLAG-tagged TMP21 resulted in a slight increase in expression levels of full-length proteins (Fig. 2A). A similar minor increase was observed for APP-CTF immunoreactivity in cells overexpressing APP-WT protein. This finding is consistent with previous investigations that demonstrated dual effects of TMP21 on  $\gamma$ -secretase activity and APP trafficking (26, 27, 30). However, unique effects in  $\gamma$ -cleavage were observed in cells co-expressing the APP $\epsilon$  construct with TMP21. Immunoprecipitation and reprobing with an anti-A $\beta$  antibody (6E10 N-terminal epitope) revealed the expected APP-CTF for the wild-type protein (Fig. 2B, short exposure, *top panel*). Upon longer exposure, two intracellular A $\beta$ -reactive bands were observed in cells expressing APP $\epsilon$  at higher molecular weights than are seen for the synthetic A $\beta$ 40 peptide (Fig. 2B, long exposure, *bottom panel*). These A $\beta$ -reactive bands accumulated in the cells co-expressing TMP21. These bands were only observed after immunoprecipitation followed by Western blotting, suggesting that they are a small percentage of the total A $\beta$ -related species.

The appearance of these bands suggests that after extracellular cleavage ( $\beta$ ,  $\beta'$ , or  $\alpha$  cleavage) the  $\gamma$ -secretase is impaired by TMP21 expression, leading to unprocessed intracellular A $\beta$  species terminating at the  $\epsilon$ -site (corresponds to A $\beta$  residue 49). The molecular weights of these TMP21-induced bands are in the range of  $\beta$ -to- $\epsilon$  A $\beta$  (residues 1–49; molecular mass, 5.3 kDa) and possibly a  $\beta'$ -to- $\epsilon$  fragment (residues 11–49; molecular mass, 4.1 kDa). These fragments also contained the A $\beta$  N terminus as shown by their reactivity to different antibodies. A $\beta$ -positive species were isolated by immunoprecipitation from cells expressing APP $\epsilon$  and probed with antibodies recognizing A $\beta$  residues 1–17 (6E10) and 17–24 (4G8). The higher molecular weight bands induced by TMP21 expression were detected by both antibodies and were not seen in control mock-transfected cells (Fig. 3, A and B). These data suggest that the bands are produced by normal cleavage at or near the  $\beta$ -secretase site and their higher molecular weight as compared with A $\beta$ -(1–40) would be consistent with impaired  $\gamma$ -processing in the presence of TMP21. The molecular

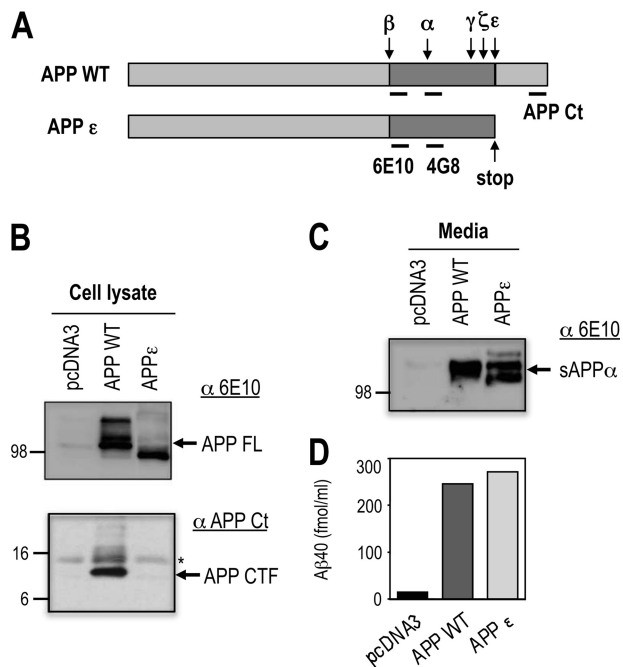


**FIGURE 1. Characterization of the APP $\epsilon$  construct.** A, schematic representation of the wild-type human amyloid- $\beta$  precursor protein (APP $^{WT}$ ) and its cleavage sites by the indicated secretases. APP $\epsilon$  corresponds to the N-terminal fragment of APP generated by  $\epsilon$ -cleavage (APP $\epsilon$ ). 6E10 antibody recognizes the 1–17 sequence of A $\beta$ , 4G8 antibody recognizes the 17–24 sequence of A $\beta$ , and APP C-terminal antibody recognizes the cytoplasmic tail. B, HEK293 cells were transiently transfected with APP $^{WT}$  or APP $\epsilon$  cDNA as described and analyzed by Western blot for detection of APP full-length (APP FL) or the APP C-terminal fragment (APP CTF) using different APP antibodies (6E10, APP CTF). The APP-CTF-directed antibody does not label APP $\epsilon$ , which lacks the C terminus. C, medium of HEK293 cells transfected with APP $^{WT}$  or APP $\epsilon$  cDNA were analyzed by immunoblotting to detect the secreted extracellular fragment soluble APP $\alpha$  using 6E10 antibody. D, level of secreted A $\beta$ 40 peptide were analyzed by ELISA from medium of HEK293 cells transfected with APP $^{WT}$  or APP $\epsilon$  cDNA.

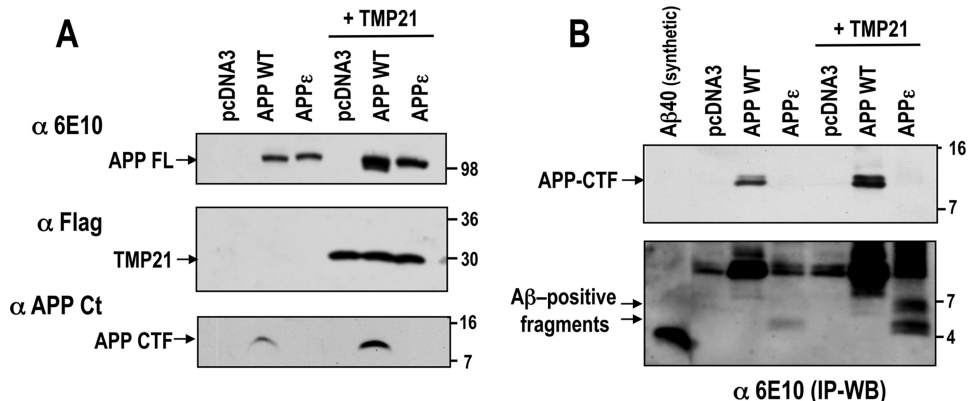


**FIGURE 2. TMP21-induced accumulation of intracellular A $\beta$ -positive fragments in cells expressing APP $\epsilon$ .** A, HEK293 cells were transiently co-transfected with TMP21-FLAG and APP $^{WT}$  or APP $\epsilon$  cDNA, then analyzed by Western blot for detection of full-length APP (APP FL), the APP C-terminal fragment (APP CTF), or TMP21-FLAG protein. B, intracellular A $\beta$  species were immunoprecipitated using 6E10 antibody (IP WB) in HEK293 cells transiently co-transfected with TMP21-FLAG along with APP $^{WT}$  or APP $\epsilon$  cDNA, then detected by Western blot using 6E10 antibody (short exposure, *top panel*). Note the high molecular weight intracellular A $\beta$  at  $\sim$ 5 kDa recognized by 6E10 antibody in cells overexpressing APP $\epsilon$  and A $\beta$ -positive bands at  $\sim$ 6.5 and 5 kDa protected by co-transfection with TMP21 (longer exposure, *bottom panel*). Synthetic A $\beta$ 40 peptide was used as a molecular weight marker and positive control.

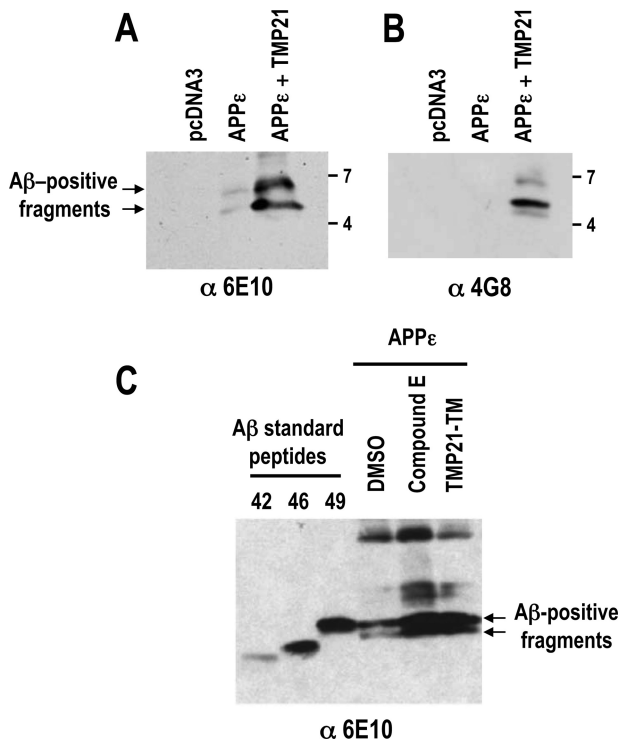


**FIGURE 3. Intracellular A $\beta$ -positive fragments are generated by impaired  $\gamma$ -processing and migrate at the level of A $\beta$ 1–49 synthetic peptides.** Intracellular A $\beta$  species were immunoprecipitated from membrane fractions using 6E10 antibody (6E10) in HEK293 cells transiently co-transfected with APP $\epsilon$  in the presence and absence of TMP21-FLAG, then detected by immunoblotting using 6E10 (A) or 4G8 (B) antibodies. C, HEK293 cells were transfected with APP $\epsilon$  in the presence or absence of TMP21-TM, then treated or not with Compound E (100 nM). Intracellular A $\beta$  species were then immunoprecipitated and detected using 6E10 antibody. Both TMP21-TM overexpression and Compound E treatment led to an accumulation of A $\beta$ -positive fragment. Synthetic A $\beta$  standard peptides were used as molecular weight markers.

weights of the bands are comparable with that of a synthetic A $\beta$  1–49 peptide, which indicates that the A $\beta$ -positive fragments would be consistent with an incompletely processed A $\beta$ -containing APP $\epsilon$  fragments (Fig. 3C). Similar bands were also observed in cells expressing the APP $\epsilon$  isoform when treated with the  $\gamma$ -secretase inhibitor, Compound E, which supports the possibility that they are generated by impaired  $\gamma$ -processing (Fig. 3C).

The fact that these fragments contain the hydrophobic terminus of A $\beta$  was supported by fractionation studies. Membrane and soluble cytosolic fractions from cells expressing APP $\epsilon$  with or without TMP21 were isolated, and the A $\beta$ -positive species were immunoprecipitated. It should be noted that APP $\epsilon$  is recovered in the membrane fraction, in agreement with the demonstration that APP $\epsilon$  behaved as a membrane-bound type 1 protein as does  $\beta$ APP (28). Probing with anti-A $\beta$  (6E10) revealed the presence in the membrane fraction but not in the soluble fraction of the high molecular weight, presumably unprocessed fragments that were induced by TMP21 expression (Fig. 4). These findings support the fact that the fragments are membrane-embedded and, therefore, likely contain the APP transmembrane domain terminating at the  $\epsilon$ -cleavage site (*i.e.* A $\beta$ 49).

Taken together, these findings indicate that in the absence of any rate-limiting  $\epsilon$ -cleavage, TMP21 has a unique effect on

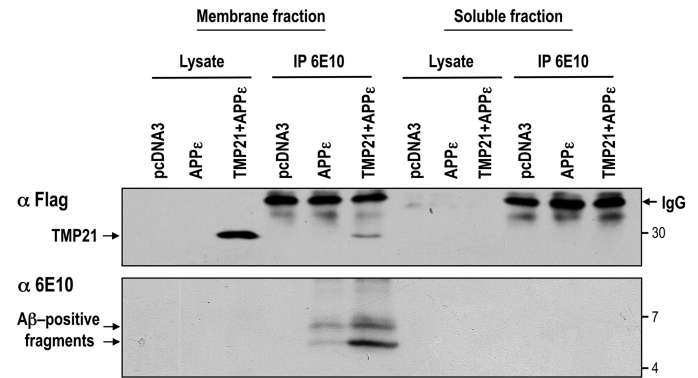


**FIGURE 4. TMP21-induced A $\beta$  species are associated with the lipid bilayer.** HEK293 cells were transiently transfected with the APP $\epsilon$  vector in the presence or absence of wild-type TMP21. Empty vector (pcDNA3) was used as a negative control. Membrane and cytosolic soluble fractions were prepared and probed with anti-FLAG antibodies for TMP21 detection or immunoprecipitated (IP) using anti-A $\beta$  6E10 and analyzed for detection of intracellular A $\beta$  species. Both TMP21 and A $\beta$  positive fragments were embedded in the membrane. No TMP21 or A $\beta$ -species were detected in the soluble fraction.

$\gamma$ -secretase activity, resulting in the accumulation of intracellular membrane-embedded A $\beta$ -related species. These results are reminiscent of recent reports describing an accumulation of intracellular longer A $\beta$  species when  $\gamma$ -secretase activity is inhibited at the  $\gamma$  site but not at the  $\epsilon$  site (31–33). TMP21-mediated  $\gamma$ -secretase inhibition was seen only with the APP $\epsilon$  construct, and no significant level of membrane-embedded A $\beta$ -reactive fragments was observed with the co-expression of APP-WT and TMP21. This suggests that one of the main targets for TMP21 may be the membrane-embedded A $\beta$  fragment (residues 1–49) that is generated after release of the AICD cytoplasmic tail. In addition, this finding provides a reporter assay to investigate which domains are responsible for its activity.

**Identification of TMP21 Functional Domains**—The TMP21-related and homologous cargo protein, p24a, was found to be inactive with respect to regulating  $\gamma$ -secretase activity (26). Therefore, p24a protein was used to create a series of chimera proteins to identify which domains of TMP21 modulate  $\gamma$ -secretase activity as seen in the APP $\epsilon$  reporter assay. Chimeras are all FLAG-tagged and included substitution of the transmembrane (TM) and C terminus of TMP21 into p24a (TMP21-TMct), replacement of the p24a N terminus with the corresponding extracellular domain of TMP21 (TMP21-Nt), replacement of p24a TM with TMP21 (TMP21-TM), and a final construct in which the TMP21 C terminus was inserted into full-length p24a (TMP21-Ct) (Fig. 5A).

The chimeras as well as wild-type TMP21 and p24a were transiently expressed in HEK293 cells, and no effects were observed on the levels of  $\gamma$ -secretase components on the levels of nicastrin maturation or PS1 processing (Fig. 5B). The chimeras all expressed at reasonable levels, suggesting that they were not misfolded or rapidly degraded. Two of the constructs, TMP21-TMct and TMP21-TM, were found at slightly higher levels as compared with wild-type TMP21 and may, therefore, be well tolerated by the cells. Co-immunoprecipitation studies were conducted for the FLAG-tagged proteins, which successfully pulled down all of the chimeras (Fig. 5C). FLAG-tagged wild-type TMP21 and p24a were used as controls, and as previously reported, TMP21 but not p24a interacts with mature

## TMP21 Functional Domain

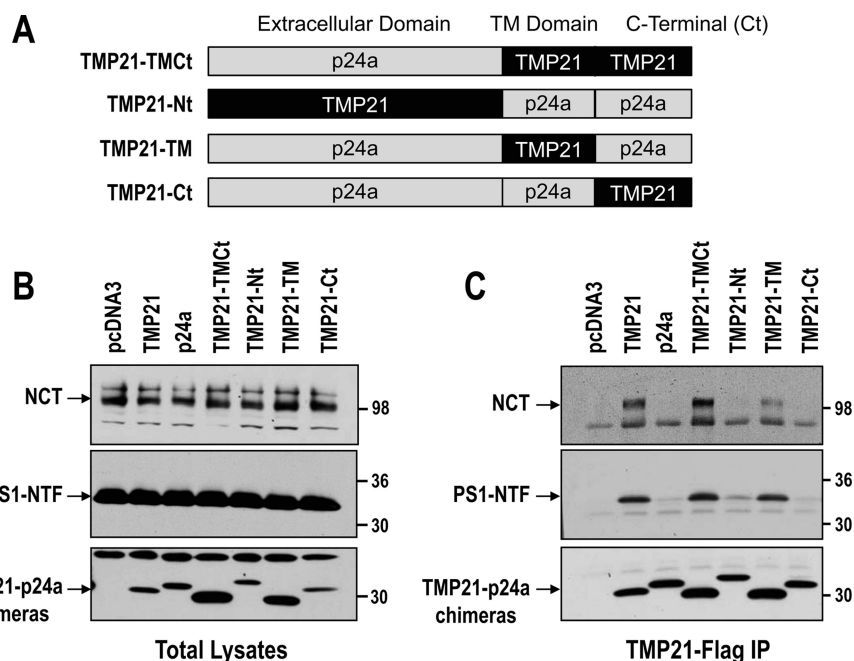


**FIGURE 5. TMP21 interacted with PS-complex through its transmembrane domain.** *A*, schematic representation of TMP21-p24a chimera FLAG-tagged proteins indicating the domains (extracellular, TM, and C terminus) of the p24a template, which were replaced with the corresponding TMP21 sequences. *B*, HEK293 cells were transiently transfected with TMP21, p24a, or chimera proteins. Membrane fractions were prepared and analyzed by Western blot for detection of NCT, PS1-NTF, and FLAG-tagged proteins. *C*, FLAG-tagged wild-type TMP21-p24a and chimeras were immunoprecipitated (IP) from membrane fractions and analyzed by immunoblotting for detection of NCT, PS1 N-terminal fragment (PS1-NTF), and the FLAG-tagged proteins. Note that only wild-type TMP21 and chimera FLAG proteins containing the transmembrane domain of TMP21 were associated with both NCT and PS1-NTF.

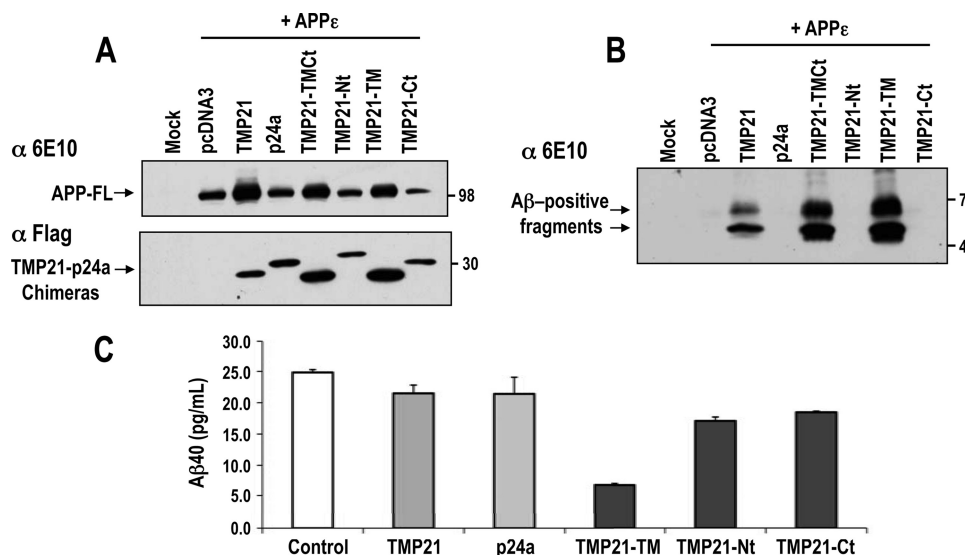


**FIGURE 6. A $\beta$  production and effects of individual TMP21 domains.** *A*, HEK293 cells were transiently co-transfected with TMP21-FLAG and APP $\epsilon$ . Membrane fraction were prepared and analyzed by Western blot for detection of APP holoprotein (APP-FL) and TMP21-FLAG proteins. *B*, intracellular A $\beta$  species were immunoprecipitated using 6E10 antibody in HEK293 cells transiently co-transfected with TMP21-FLAG and APP $\epsilon$  and subsequently probed with the 6E10 antibody. Only TMP21 and chimera FLAG proteins containing the transmembrane domain of TMP21 resulted in the accumulation of the membrane-embedded higher molecular weight A $\beta$ -positive fragments. *C*, HEK293 cells were co-transfected with APP $\epsilon$  and TMP1-p24a chimeras, and A $\beta$ 40 levels were determined by ELISA. No changes were observed for full-length TMP21 or p24a and chimeras containing the extracellular N terminus (TMP21-Nt) or intracellular C terminus (TMP21-Ct) of TMP21. Significant reduction was observed for cells expressing the chimera containing the TMP21 transmembrane domain (TMP21-TM).

NCT and the PS1-NTF (Fig. 5C). However, significant differences were observed between the chimeras. Association with mature NCT and the PS1-NTF were only found for con-

structs containing the TM domain of TMP21 (TMP21-TMct and TMP21-TM; Fig. 5C). In contrast, no binding was observed for chimera containing the N- or C-terminal fragments of TMP21. These observations indicate that the transmembrane domain of TMP21 is essential for its physical interaction with the  $\gamma$ -secretase complex and may be the primary site of action.

To investigate their functional aspects, TMP21 chimeras were co-transfected with APP $\epsilon$ . Full-length APP $\epsilon$  was found to be expressed at higher levels for cells co-transfected with wild-type TMP21 or the chimeras TMP21-TMct or TMP21-TM, containing the transmembrane domain (Fig. 6A). This phenomenon may be the result of the effect of TMP21 on APP trafficking as noted previous (30). Examination of the intracellular A $\beta$ -containing fragments by immunoprecipitation followed by Western blotting revealed that the two higher molecular weight species were only seen for the chimeras containing the TMP21 transmembrane domain (TMP21, TMP21-TMct, and TMP21-TM, Fig. 6B). This is consistent with the observed interactions of the chimeras with PS1 and NCT which were dependent upon the TMP21 TM domain. The relative intensity of A $\beta$ -positive fragments observed in cells expressing TMP21-TMct and TMP21-TM chimeras was higher than for the wild-type TMP21. This could be because of slightly higher levels of the chimeras, as FLAG immunoreactivities were more pronounced (Fig. 6A). Alternatively, this may reflect the fact that the chimeric proteins were more readily or efficiently incorporated into the  $\gamma$ -secretase complexes. Only a small proportion of the full-length TMP21 is incorporated into complexes, and therefore, replacement, for example, of the ectodomain in the chimeras may result in a more accessible conformation for secretase binding.

Appearance of the A $\beta$ -positive fragments suggests that they may result from a decreased processing of the APP-CTF. It would, therefore, be predicted that a corresponding decrease in

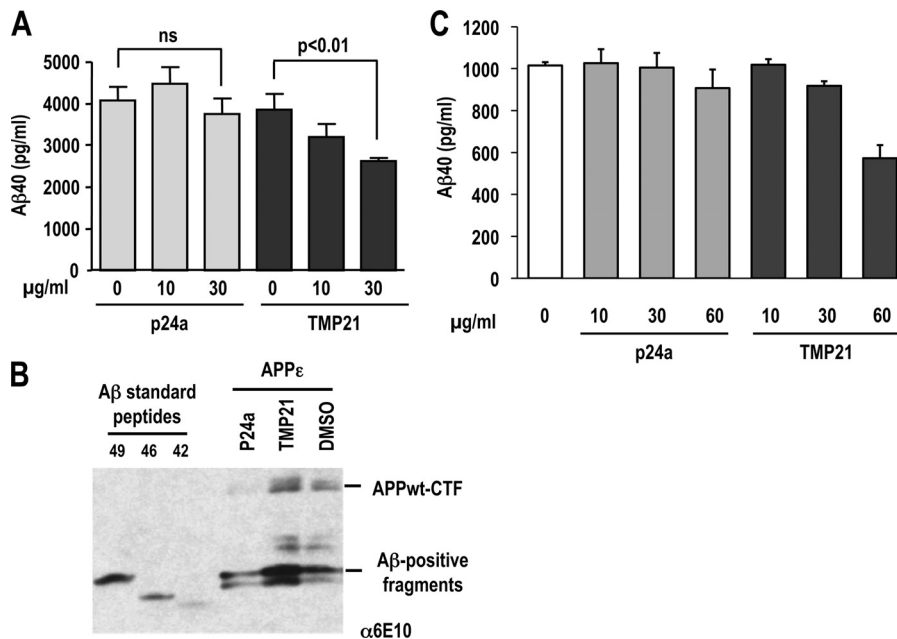


**FIGURE 7. Synthetic transmembrane domain of TMP21 reduced A $\beta$ 40 secretion.** *A*, HEK293 cells stably overexpressing APP<sup>sw</sup> were treated with the synthetic transmembrane domain of TMP21 or p24a (0, 10, 30  $\mu$ g/ml), and levels of secreted A $\beta$ 40 peptide were analyzed by ELISA after 8 h of incubation. The synthetic peptide corresponding to the TMP21 transmembrane domain decreased A $\beta$ 40 processing and secretion in a dose-dependent manner. No significant effects were observed for the related p24a TM domain peptide. *B*, HEK293 cells were transfected with APP $\epsilon$ , and 8 h before harvesting cells were treated with TMP21 or p24a transmembrane peptides (30  $\mu$ g/ml) or a DMSO control. Intracellular A $\beta$  species were immunoprecipitated and detected using 6E10 antibody. Treatment with the TMP21-TM peptide only resulted in the accumulation of A $\beta$ -positive fragments. Synthetic A $\beta$  standard peptides were used as molecular weight markers confirmed that the fragments had molecular weights corresponding to A $\beta$ 1–49 and related peptides. *C*, cell-free assays were conducted using membrane preparations from HEK293 cells with recombinant APP-C100 as the  $\gamma$ -secretase substrate. Synthetic peptides corresponding to transmembrane domains of TMP21 and p24a were added to final concentrations of 0, 10, 30, and 60  $\mu$ g/ml to the reaction mixture.

A $\beta$  secretion would be seen under these conditions. However, a more complex response was associated with TMP21 and the chimera proteins with respect to A $\beta$  production. Overexpression of full-length wild-type TMP21 and APP $\epsilon$  did not result in any significant change in A $\beta$  production (Fig. 6C). Levels were comparable with controls as well as cell transfected with the p24a homolog. This is consistent with other studies in whole cells where high levels of TMP21 were also shown to not have an appreciable effect on A $\beta$  levels (26, 27). Therefore, the A $\beta$ -positive fragments must represent only a small percentage of the total A $\beta$ . This could be because of a limited incorporation of full-length TMP21 into mature complexes. Similar issues with incorporation into functional complexes are seen for NCT, which is also not readily assembled into active complexes and accumulates as the immature species.

For the chimera proteins, expression of constructs containing the N-terminal ectodomain (TMP21-Nt) or the intracellular cytoplasmic tail (TMP21-Ct) did not result in any appreciable changes in A $\beta$  production (Fig. 6C). In contrast, expression of the chimera containing the TMP21 transmembrane domain (TMP21-TM) with APP $\epsilon$  reduced A $\beta$  levels by  $\sim$ 65% (Fig. 6C). The double-chimera TMP21-TMct also reduced A $\beta$  levels below that of the TMP21-Nt and TMP21-Ct constructs, consistent with their binding to PS1 and NCT (data not shown). The ability of the TMP21-TM-containing chimera was a consistent observation which suggests that the transmembrane domain has a more pronounced effect than full-length TMP21.

The reason for this is unclear, but it is possible that the other domains (N and C termini) regulate other functions such as trafficking or binding to the  $\gamma$ -secretase complex. Therefore, replacement of these domains may result in a more potent activity of the TMP21 transmembrane region.

TM-containing chimeras binding to the  $\gamma$ -complex may represent one of their mechanisms of action. However, the chimeras also consistently increased the levels of full-length APP $\epsilon$  precursor. This could provide another explanation for the accumulation of the A $\beta$ -positive fragments and possibly changes in A $\beta$  levels. Based upon these observations, either of the two functional aspects of TMP21, inhibition of  $\gamma$ -secretase cleavage or changes in APP metabolism, may be responsible for the alterations in A $\beta$ -related processing (26, 27, 30). To try and dissect these two functions, direct interaction of the TMP21 transmembrane domain to the  $\gamma$ -secretase complex and its ability to alter cleavage were investigated using synthetic peptides in

cell culture and cell-free assays.

*Effects of a Synthetic Transmembrane Domain on A $\beta$  Processing*—The TM domains of TMP21 and p24a were synthesized with three additional lysine residues attached at both the N and C termini to increase solubility. This approach has been used previously for investigations into the membrane insertion and structure of the APP transmembrane helix (34). The TMP21 TM peptide (KKK-VLYFSIFSMFCLIGLATWQV-FYL-KKK) solubilized in DMSO was added at different concentrations to cells expressing the APP-Swedish variant, and A $\beta$ 40 secretion was measured in medium by ELISA analysis. After incubation for 8 h, cells exposed to 10  $\mu$ g/ml (final media concentration) of the TMP21 peptide reduced A $\beta$ 40 by  $\sim$ 17% (Fig. 7A). A dose response was observed at 30  $\mu$ g/ml peptide which produced an  $\sim$ 32% reduction in A $\beta$  secretion. The corresponding p24a transmembrane peptide (KKK-VVLSFFEALVLVAMTLGQIYYL-KKK) had no statistically significant effects at either 10 or 30  $\mu$ g/ml (Fig. 7A). The reduction of A $\beta$  levels was also not because of an inherently toxic effect of the TMP21 peptide that may have led to loss of production because of cell death. Viability assays indicated that no cell toxicity was associated with either the TMP21 or p24a peptides at the concentrations investigated (supplemental Fig. 1). The reduced A $\beta$ 40 trend for cells treated with the TMP21 peptide at longer conditioning time (e.g. 16 h) remained the same with comparable dose-dependent decreases for treatments with 10 and 30  $\mu$ g/ml (data not shown). Treatment of cells expressing APP $\epsilon$  with the

## TMP21 Functional Domain

TMP21-TM synthetic peptide demonstrated a similar increase in the antibody-positive fragments (Fig. 7B). These fragments were identical to those seen after transfection of the TMP21-TM construct or wild-type protein. No change in these antibody-positive fragments was observed after treatment with the comparable p24a-TM peptide or DMSO control (Fig. 7B). These observations suggest that, in addition to its effects on APP metabolism, TMP21 can directly alter  $\gamma$ -secretase activity. Given the specific ability of the synthetic TMP21 transmembrane domain to decrease A $\beta$ 40 production, it is likely that the peptide associates with the  $\gamma$ -secretase complex and reduces proteolysis. These observations are consistent with the effects of recombinant TMP21 on A $\beta$  processing as shown previously (26).

Cell-free  $\gamma$ -secretase assays were also conducted in an effort to support these findings and investigate the activity of the synthetic TM peptides. Membrane fractions were prepared from HEK293 cells and incubated with the synthetic TM peptides at various concentrations. Recombinant C100 protein was added to the reaction mixture, and A $\beta$  production was assayed by ELISA. Incubation of membranes with the TMP21 or p24a transmembrane peptides at 10  $\mu$ g/ml did not have any detectable effect on A $\beta$  levels (Fig. 7C). The TMP21 peptide had a modest effect at 30  $\mu$ g/ml which resulted in approximately a 10% reduction in A $\beta$  production (Fig. 7C). A more pronounced decrease in A $\beta$  was observed for membranes incubated with 60  $\mu$ g/ml of the TMP21 TM peptide which resulted in an ~50% reduction in A $\beta$  processing. This was specific for the TMP21 peptide, as no significant difference was observed for the corresponding p24a TM peptide (Fig. 7C).

Relatively higher concentrations of the TMP21 transmembrane peptide were required in the cell-free assay to produce the same decrease in A $\beta$  processing as compared with the live cell cultures. This may be because of the fact that the level of the C100 substrate is much higher in the cell-free assay. Therefore, if the TMP21 binds to the  $\gamma$ -secretase complex as proposed, then the higher amount of substrate could compete for binding sites in the  $\gamma$ -complex. As a result, increased amounts of the TMP21 transmembrane peptide would be required to displace and/or compete with the C100 substrate.

Taken together, these observations have demonstrated that TMP21 expression has a unique effect on  $\gamma$ -secretase processing when examined in the absence of a possibly competing  $\epsilon$ -mediated proteolysis. This was evident by the effects seen with the truncated APP $\epsilon$  which led to the accumulation of A $\beta$ -containing membrane-embedded fragments. Because the AICD sequence, which is lacking in APP $\epsilon$  construct, contains the YENP motif, essential for APP internalization (35), it is possible to envisage that TMP21 acts on  $\gamma$ -secretase activity and upstream APP recycling and preferentially targets the membrane-embedded A $\beta$  fragment released after the  $\epsilon$ -cleavage. However, this remains speculative, and the exact site of the twin function of TMP21 in terms of  $\gamma$ -secretase modulation and APP metabolism has yet to be elucidated. The direct activity of TMP21 on  $\gamma$ -secretase appeared to be primarily mediated by its transmembrane domain. It is likely that specific residues are responsible for these effects, and further mutagenesis studies may shed more light on this issue. However, the ability of the TMP21 peptide to alter APP processing and A $\beta$  production

could represent a novel strategy for modulating amyloid production and its subsequent pathology.

## REFERENCES

1. Vardy, E. R., Catto, A. J., and Hooper, N. M. (2005) *Trends Mol. Med.* **11**, 464–472
2. Weidemann, A., Eggert, S., Reinhard, F. B., Vogel, M., Paliga, K., Baier, G., Masters, C. L., Beyreuther, K., and Evin, G. (2002) *Biochemistry* **41**, 2825–2835
3. Baek, S. H., Ohgi, K. A., Rose, D. W., Koo, E. H., Glass, C. K., and Rosenfeld, M. G. (2002) *Cell* **110**, 55–67
4. von Rotz, R. C., Kohli, B. M., Bosset, J., Meier, M., Suzuki, T., Nitsch, R. M., and Konietzko, U. (2004) *J. Cell Sci.* **117**, 4435–4448
5. Kim, H. S., Kim, E. M., Lee, J. P., Park, C. H., Kim, S., Seo, J. H., Chang, K. A., Yu, E., Jeong, S. J., Chong, Y. H., and Suh, Y. H. (2003) *FASEB J.* **17**, 1951–1953
6. Ryan, K. A., and Pimplikar, S. W. (2005) *J. Cell Biol.* **171**, 327–335
7. Pardossi-Piquard, R., Petit, A., Kawarai, T., Sunyach, C., Alves da Costa, C., Vincent, B., Ring, S., D'Adamio, L., Shen, J., Müller, U., St. George-Hyslop, P., and Checler, F. (2005) *Neuron* **46**, 541–554
8. Pardossi-Piquard, R., Dunys, J., Yu, G., St. George-Hyslop, P., Alves da Costa, C., and Checler, F. (2006) *J. Neurochem.* **97**, 1052–1056
9. Alves da Costa, C., Sunyach, C., Pardossi-Piquard, R., Sévalle, J., Vincent, B., Boyer, N., Kawarai, T., Girardot, N., St. George-Hyslop, P., and Checler, F. (2006) *J. Neurosci.* **26**, 6377–6385
10. Zhang, Y. W., Wang, R., Liu, Q., Zhang, H., Liao, F. F., and Xu, H. (2007) *Proc. Natl. Acad. Sci. U.S.A.* **104**, 10613–10618
11. Liu, Q., Zerbiniatti, C. V., Zhang, J., Hoe, H. S., Wang, B., Cole, S. L., Herz, J., Muglia, L., and Bu, G. (2007) *Neuron* **56**, 66–78
12. Rogaev, E. I., Sherrington, R., Rogaeva, E. A., Levesque, G., Ikeda, M., Liang, Y., Chi, H., Lin, C., Holman, K., Tsuda, T., et al. (1995) *Nature* **376**, 775–778
13. Sherrington, R., Rogaev, E. I., Liang, Y., Rogaeva, E. A., Levesque, G., Ikeda, M., Chi, H., Lin, C., Li, G., Holman, K., et al. (1995) *Nature* **375**, 754–760
14. Yu, G., Nishimura, M., Arawaka, S., Levitan, D., Zhang, L., Tandon, A., Song, Y. Q., Rogaeva, E., Chen, F., Kawarai, T., Supala, A., Levesque, L., Yu, H., Yang, D. S., Holmes, E., Milman, P., Liang, Y., Zhang, D. M., Xu, D. H., Sato, C., Rogaev, E., Smith, M., Janus, C., Zhang, Y., Aebbersold, R., Farrer, L. S., Sorbi, S., Bruni, A., Fraser, P., and St. George-Hyslop, P. (2000) *Nature* **407**, 48–54
15. Francis, R., McGrath, G., Zhang, J., Ruddy, D. A., Sym, M., Apfeld, J., Nicoll, M., Maxwell, M., Hai, B., Ellis, M. C., Parks, A. L., Xu, W., Li, J., Gurney, M., Myers, R. L., Himes, C. S., Hiesch, R., Ruble, C., Nye, J. S., and Curtis, D. (2002) *Dev. Cell* **3**, 85–97
16. De Strooper, B., Saftig, P., Craessaerts, K., Vanderstichele, H., Guhde, G., Annaert, W., Von Figura, K., and Van Leuven, F. (1998) *Nature* **391**, 387–390
17. Kimberly, W. T., LaVoie, M. J., Ostaszewski, B. L., Ye, W., Wolfe, M. S., and Selkoe, D. J. (2003) *Proc. Natl. Acad. Sci. U.S.A.* **100**, 6382–6387
18. Takasugi, N., Tomita, T., Hayashi, I., Tsuruoka, M., Niimura, M., Takahashi, Y., Thinakaran, G., and Iwatsubo, T. (2003) *Nature* **422**, 438–441
19. Edbauer, D., Winkler, E., Regula, J. T., Pesold, B., Steiner, H., and Haass, C. (2003) *Nat. Cell Biol.* **5**, 486–488
20. Gu, Y., Chen, F., Sanjo, N., Kawarai, T., Hasegawa, H., Duthie, M., Li, W., Ruan, X., Luthra, A., Mount, H. T., Tandon, A., Fraser, P. E., and St. George-Hyslop, P. (2003) *J. Biol. Chem.* **278**, 7374–7380
21. Gu, Y., Sanjo, N., Chen, F., Hasegawa, H., Petit, A., Ruan, X., Li, W., Shier, C., Kawarai, T., Schmitt-Ulms, G., Westaway, D., St. George-Hyslop, P., and Fraser, P. E. (2004) *J. Biol. Chem.* **279**, 31329–31336
22. Thinakaran, G., Borchelt, D. R., Lee, M. K., Slunt, H. H., Spitzer, L., Kim, G., Ratovitsky, T., Davenport, F., Nordstedt, C., Seeger, M., Hardy, J., Levey, A. I., Gandy, S. E., Jenkins, N. A., Copeland, N. G., Price, D. L., and Sisodia, S. S. (1996) *Neuron* **17**, 181–190
23. Wolfe, M. S., Xia, W., Ostaszewski, B. L., Diehl, T. S., Kimberly, W. T., and Selkoe, D. J. (1999) *Nature* **398**, 513–517
24. Chen, F., Yu, G., Arawaka, S., Nishimura, M., Kawarai, T., Yu, H., Tandon, A., Supala, A., Song, Y. Q., Rogaeva, E., Milman, P., Sato, C., Yu, C., Janus,

- C., Lee, J., Song, L., Zhang, L., Fraser, P. E., and St. George-Hyslop, P. H. (2001) *Nat. Cell Biol.* **3**, 751–754
25. Shah, S., Lee, S. F., Tabuchi, K., Hao, Y. H., Yu, C., LaPlant, Q., Ball, H., Dann, C. E., 3rd, Südhof, T., and Yu, G. (2005) *Cell* **122**, 435–447
  26. Chen, F., Hasegawa, H., Schmitt-Ulms, G., Kawai, T., Böhm, C., Katayama, T., Gu, Y., Sanjo, N., Glista, M., Rogaeva, E., Wakutani, Y., Pardossi-Piquard, R., Ruan, X., Tandon, A., Checler, F., Marambaud, P., Hansen, K., Westaway, D., St. George-Hyslop, P., and Fraser, P. (2006) *Nature* **440**, 1208–1212
  27. Dolcini, V., Dunys, J., Sevalle, J., Chen, F., Guillot-Sestier, M. V., St. George-Hyslop, P., Fraser, P. E., and Checler, F. (2008) *Biochem. Biophys. Res. Commun.* **371**, 69–74
  28. Lefranc-Jullien, S., Sunyach, C., and Checler, F. (2006) *J. Neurochem.* **97**, 807–817
  29. Blum, R., Feick, P., Puype, M., Vandekerckhove, J., Klengel, R., Nastainczyk, W., and Schulz, I. (1996) *J. Biol. Chem.* **271**, 17183–17189
  30. Vetrivel, K. S., Gong, P., Bowen, J. W., Cheng, H., Chen, Y., Carter, M., Nguyen, P. D., Placanica, L., Wieland, F. T., Li, Y. M., Kounnas, M. Z., and Thinakaran, G. (2007) *Mol. Neurodegener.* **2**, 4
  31. Qi-Takahara, Y., Morishima-Kawashima, M., Tanimura, Y., Dolios, G., Hirotsu, N., Horikoshi, Y., Kametani, F., Maeda, M., Saido, T. C., Wang, R., and Ihara, Y. (2005) *J. Neurosci.* **25**, 436–445
  32. Ren, Z., Schenk, D., Basi, G. S., and Shapiro, I. P. (2007) *J. Biol. Chem.* **282**, 35350–35360
  33. Zhao, G., Mao, G., Tan, J., Dong, Y., Cui, M. Z., Kim, S. H., and Xu, X. (2004) *J. Biol. Chem.* **279**, 50647–50650
  34. Gorman, P. M., Kim, S., Guo, M., Melnyk, R. A., McLaurin, J., Fraser, P. E., Bowie, J. U., and Chakrabarty, A. (2008) *BMC Neurosci.* **9**, 17
  35. King, G. D., and Scott Turner, R. (2004) *Exp. Neurol.* **185**, 208–219
  36. Grandori, R., Struck, K., Giovanielli, K., and Carey, J. (1997) *Protein Eng.* **10**, 1099–1100